TISSUE ENGINEERING: Part C
Volume 18, Number 11, 2012

DOI: 10.1089/ten.tec.2011.0624

In Vitro Differentiation and Mineralization of Dental Pulp Stem Cells on Enamel-Like Fluorapatite Surfaces

Xiaodong Wang, Ph.D.,[1,2] Taocong Jin, M.D.,[2] Syweren Chang, M.S.,[2]
Zhaocheng Zhang, Ph.D.,[2] Agata Czajka-Jakubowska, Ph.D.,[3] Jacques E. Nör, Ph.D.,[2]
Brian H. Clarkson, Ph.D.,[2] Longxing Ni, Ph.D.,[1] and Jun Liu, Ph.D.[2]

Our previous studies have shown good biocompatibility of fluorapatite (FA) crystal surfaces in providing a favorable environment for functional cell–matrix interactions of human dental pulp stem cells (DPSCs) and also in supporting their long-term growth. The aim of the current study was to further investigate whether this enamel-like surface can support the differentiation and mineralization of DPSCs, and, therefore, act as a potential model for studying the enamel/dentin interface and, perhaps, dentine/pulp regeneration in tooth tissue engineering. The human pathway-focused osteogenesis polymerase chain reaction (PCR) array demonstrated that the expression of osteogenesis-related genes of human DPSCs was increased on FA surfaces compared with that on etched stainless steel (SSE). Consistent with the PCR array, FA promoted mineralization compared with the SSE surface with or without the addition of a mineralization promoting supplement (MS). This was confirmed by alkaline phosphatase (ALP) staining, Alizarin red staining, and tetracycline staining for mineral formation. In conclusion, FA crystal surfaces, especially ordered (OR) FA surfaces, which mimicked the physical architecture of enamel, provided a favorable extracellular matrix microenvironment for the cells. This resulted in the differentiation of human DPSCs and mineralized tissue formation, and, thus, demonstrated that it may be a promising biomimetic model for dentin-pulp tissue engineering.

Introduction

Tooth loss caused by caries, periodontal diseases, trauma, and other diseases is common and seriously affects the life quality of humans. Lost teeth are traditionally replaced by artificial dentures or implants. However, artificial dentures and implants are not physiologically or biologically functional restorations of lost teeth. Recent advances in tissue engineering and stem cell biology provide an attractive prospect for dental pulp regeneration and repair of injured hard tissues such as dentin and bone.[1] For tooth or bone tissue-engineering purposes, biocompatible and bioactive scaffolds, responding mesenchymal cells, and inductive growth factors are the three key ingredients. Among all the tissue-engineering techniques, a biocompatible scaffold with appropriate chemical, physical, and mechanical properties is essential to the repair and functional regeneration of impaired tissues. Ideally, it is desirable that a scaffold should not only support the long-term growth of specific cells but also direct the differentiation of these cells toward the creation of functional tissues.

During tooth development, the formation of dentin is achieved through epithelial signal-induced differentiation of dental papilla mesenchymal cells into odontoblasts. After the eruption of a tooth, the regeneration of dentin depends on dental mesenchymal stem cells differentiating into odontoblasts. To date, a readily accessible source of such stem cells is the dental pulp: the human dental pulp stem cells (DPSCs). These cells provide, in a tissue-engineering sense, a promising approach to achieve dentin and pulp regeneration and repair. Further through interactions with the enamel-like, ordered (OR) fluorapitite (FA) crystal surfaces, eventually help to create an enamel/dentin/pulp complex because these cells are easily collected, have a rapid proliferation rate, and multiple differentiation potentials.[2,3]

Earlier, we had demonstrated a method to generate aligned FA crystal surfaces. The crystals were well aligned, and the densely packed growth mode resulted in a highly orientated enamel-like FA film.[4] We have also reported the initial cellular response of different cells to the OR and disordered (DS) FA crystal surfaces and explored the mechanisms underlying this cellular response.[5] Both the OR and DS FA surfaces were shown to have good biocompatibility and supported the long-term growth of DPSCs. We have also reported an enhanced cellular response of DPSCs to the OR

[1]Department of Operative Dentistry and Endodontics, School of Stomatology, Fourth Military Medical University, Shaanxi, P.R. China.
[2]Department of Cariology, Restorative Sciences and Endodontics, Dental School, University of Michigan, Ann Arbor, Michigan.
[3]Department of Conservative Dentistry and Periodontology, Poznan University of Medical Sciences, Poznan, Poland.

FA crystal surface, which involved a set of delicately regulated matrix and adhesion molecules. This could be further manipulated by treating the cells with a dentin inducing supplement (dentin extract), to produce a dentin/enamel superstructure.[5,6] However, we had also shown that MG-63 cells grown on the FA surface were able to differentiate and mineralize without treatment with an osteogenic induction (OI) supplement.[7] This suggested that the FA crystal films, probably through their intrinsic properties and their surface characteristics, may promote the differentiation and mineralization of dental mesenchymal stem cells without treatment by dentinal soluble molecules or by a mineralization inducing supplement.

Thus, in the present study, we aimed at investigating whether FA crystal surfaces induce and promote the differentiation and mineralization of human DPSCs and, as a result, provide a scaffold for the dentin and pulp regeneration and, potentially, a simple biomimetic model for creating an enamel/dentin/pulp complex. The human pathway-focused osteogenesis polymerase chain reaction (PCR) array was performed to detect the expression of pathway-focused osteogenesis-related molecules. To prove our hypothesis and to detect whether FA induced and promoted differentiation and mineralization, staining for alkaline phosphatase (ALP) and hard tissue formation was carried out on DPSCs cultured on FA as well as etched stainless steel (SSE) surfaces with or without a mineralization promoting supplement (MS).

Materials and Methods

Synthesis of the FA apatite surfaces

The synthesis and coating of the FA crystal on the SSE has been carried out as previously described.[4,7] Briefly, for a typical synthesis of FA crystals, 9.36 g ethylenedeiaminetetraacetic acid calcium disodium salt (EDTA-Ca-Na_2) and 2.07 g $NaH_2PO_4 \cdot H_2O$ were mixed with distilled water to a full volume of 90 mL. The suspension was continuously stirred until the powder was completely dissolved. The pH was adjusted to 6.0 using NaOH. At the same time, 0.21 g NaF was dissolved in 10 mL distilled water (pH 7.0) and continuously stirred. The two solutions were mixed, and the FA crystal growth on the substrates (15 mm 316 stainless steel discs) was achieved by adding the plates to 200 mL of newly prepared EDTA-Ca-Na_2/NaH_2PO4/NaF mixture and then autoclaving at 121°C at pressure of 2.4×10^5 Pa for 10 h. OR and DS films were synthesized separately on the under surfaces and upper surfaces of the stainless steel discs, respectively.

Cell culture and seeding

DPSCs (kindly donated by Dr. S. Shi, USC) were subcultured in Dulbecco's modified Eagle's medium (DMEM) supplemented with 10% fetal bovine serum, 100 units/mL of penicillin, and 100 μg/mL of streptomycin, maintained at 37°C in a humidified atmosphere containing 5% CO_2. Before cell seeding, the OR, DS FA, and SSE surfaces were incubated with a culture medium for 2 h. DPSCs at passage 5 were then seeded onto the different surfaces at a density of 5×10^4 cells/mL in 12-well plates under the culture conditions just described. After confluence, DPSCs were further cultured with or without treatment of MS. The medium and the supplements were replaced every 2 days.

ALP staining

After 1 week of culturing with or without MS of ascorbic acid (50 mg/mL) and β-glycerophosphate (10 mM), DPSCs grown on OR, DS, and SSE surfaces were washed with phosphate-buffered saline (PBS) and fixed in 4% paraformaldehyde for 30 min, washed 3× in dH_2O, and then incubated with 1 mg/mL Fast red TR (Sigma-Aldrich) and 0.5 mg/mL napthol AS-MX phosphate (Sigma-Aldrich) 0.1 M Tris buffer (pH 9.2) containing 1% *N*,*N* dimethylformamide (Sigma-Aldrich) for an ALP-substrate color reaction. After incubation at 37°C for 1 h, the cultures were washed twice in PBS, counterstained in 4′,6-diamidino-2-phenylindole (DAPI) (300 mM, Invitrogen) for 10 min, and then further washed twice in PBS before fluorescence imaging. Discs without cells served as controls.

Scanning electron microscope observation

After 4 weeks of culture with or without mineralization induction, the DPSCs grown on the different surfaces were rinsed and fixed in 2.5% glutaraldehyde for 1 h, dehydrated through a series of grade ethanol from 25% to 100%, and then placed in a vacuumed desiccator to dry overnight. Scanning electron microscope (SEM) analysis was conducted on a Phillips XL30FEG SEM (FEI Company) operated at 10 kV. The SEM specimen was coated with an Au/Pd film to prevent specimen charging.

Alizarin red staining and osteogenesis quantitative assay

After 4 weeks, the cells grown on three different surfaces, with or without the addition of MS, were collected for Alizarin red staining according to the manufacturer's instructions (Osteogenesis Assay Kit, Millipore). Briefly, the cells were rinsed, fixed with 70% ethanol, incubated with Alizarin red staining solution for 20 min, and washed with dH_2O 4×5 min. After staining, the quantitative analysis was carried out through the extraction of Alizarin red from stained samples using acetic acid according to the manufacturer's protocols. Three to five samples from each group were used for the Alizarin red quantification. The Alizarin red concentration was determined by the optical density value at absorbance of 405 nm. Discs without cells were also stained as controls.

RNA isolation and reverse transcription

Total cellular RNA was isolated from DPSCs grown for 4 weeks with or without MS treatment on the three different surfaces using the RNeasy Mini kit according to the manufacturer's instructions. The RNA was treated with the RNase-free DNase Set during RNA isolation. The cDNA samples were prepared from the isolated RNA using the reverse transcription (RT) first-strand kit, according to the manufacturer's protocols. An average of eight replicates of each FA crystal substrate on which the cells were grown was used for the total cellular RNA isolation and cDNA sample preparation.

RT^2 profiler PCR array analysis

The gene profile of each specimen was analyzed using the human pathway-focused osteogenesis PCR array. Briefly, the prepared cDNA samples were added to the RT^2 qPCR

master mix containing SYBR Green and reference dye. The mixture just described was then aliquoted across the PCR array templates that contain 84 human osteogenesis pathway-specific genes plus controls. The real-time PCR analysis was carried out using an ABI 7700 sequence detector (Applied Biosystems). Relative gene expression values were analyzed using the Superarray web-based software package that performed all ΔΔCt-based fold-change calculations, which sets a change of at least twofold as the "cutoff" value for the transcripts being differentially expressed in the experimental groups. Duplicate 96-well plates were used in this PCR array analyses.

In vitro *tetracycline staining*

The growth of DPSCs on FA crystal surfaces under the conditions just described was extended for an additional 2 weeks. After 6 weeks of induction, tetracycline, a bone fluorochrome was administered to label mineralized tissue formation. Briefly, the labeling medium (DMEM with 20 μg/mL

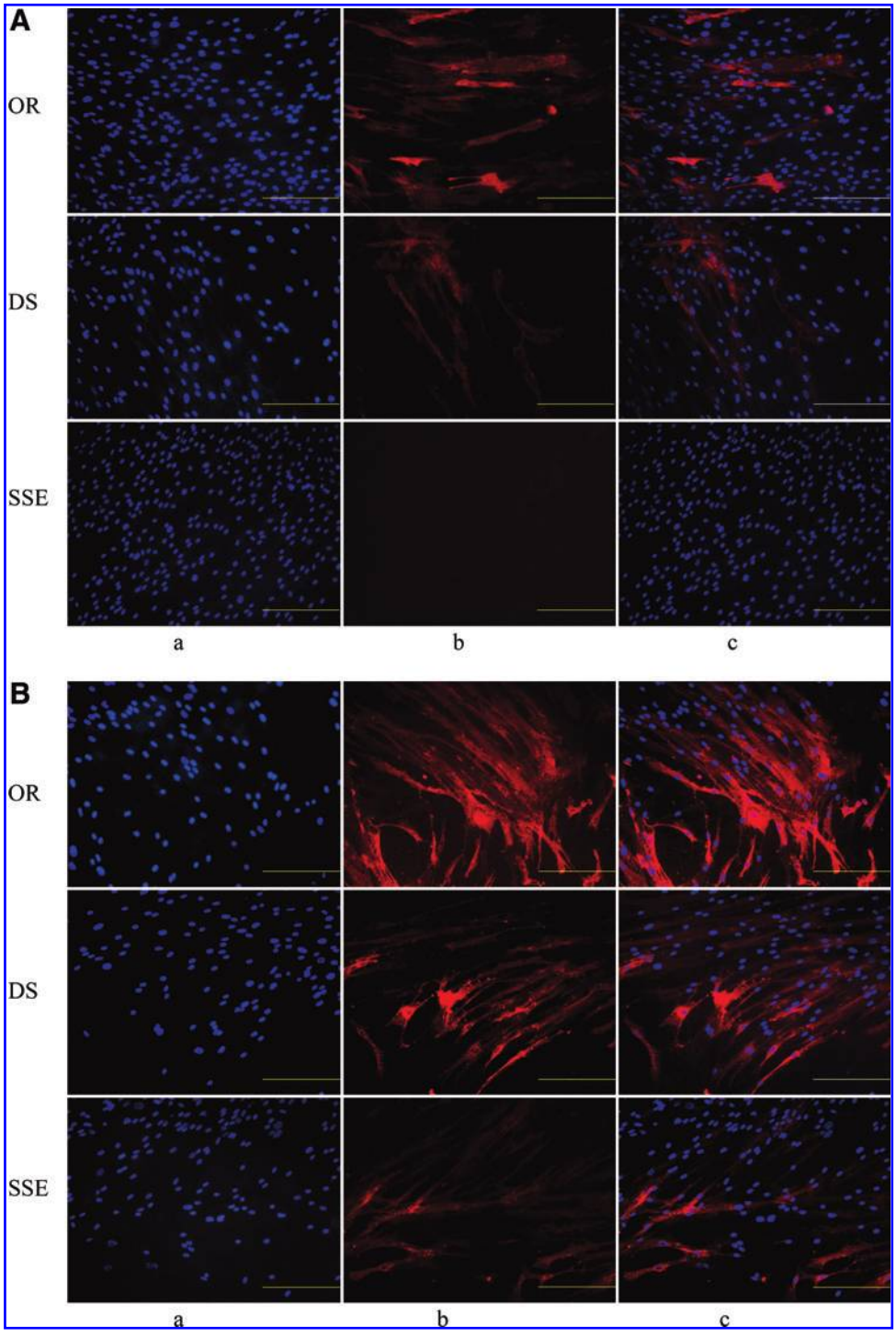

FIG. 1. ALP fluorescence staining of DPSCs grown on OR, DS FA surfaces, and SSE surfaces with or without treatment of MS for 1 week. **(A)** Without MS treatment. **(B)** With MS treatment. **(a)** DAPI nuclei staining; **(b)** ALP staining; **(c)** merged picture of **(a)** and **(b)**. Scale bar represents 200 μm. ALP, alkaline phosphatase; DPSCs, human dental pulp stem cells; OR, ordered; DS, disordered; FA, fluorapatite; SSE, etched stainless steel; MS, mineralization promoting supplement. Color images available online at www.liebertpub.com/tec

tetracycline) was freshly prepared, and then used for the last feeding of cells grown on the experimental surfaces. After staining, the discs with seeded cells were washed with DMEM, fixed in 10% neutral buffered formalin, and embedded in methyl methacrylate by routine histological methods. Serial sections of 150 μm thickness were cut from specimens with a diamond saw, and then ground and polished to approximately 10 μm using a microgrinding machine system (D-2000; Exakt-Apparatebau). The sections were then observed and imaged under fluorescence microcopy and further stained using 1% toluidine blue for histological observation. After that, the fluorescence pictures are merged with their corresponding toluidine blue staining pictures.

Statistical analysis

The osteogenesis quantitative assay results were statistically analyzed using GraphPad Prism 5 for one-way analysis of variance and Tukey's *post hoc* test of an average of three to five replicates, and significance was considered at $p < 0.05$. Data are expressed as means ± standard deviation.

Results

ALP staining

ALP-positive cells were stained red, and cell nuclei were stained blue. After 1 week, without MS treatment, a few ALP-positive cells could be seen in DPSCs grown on OR and DS surfaces. No identifiable ALP-positive staining was found in the DPSCs grown on SSE surfaces (Fig. 1A). With MS treatment, there was obvious ALP staining in all groups. However, the DPSCs grown on OR and DS surfaces displayed much stronger ALP staining compared with those on the SSE surfaces. Stronger ALP staining could also be observed in the DPSCs grown on OR surfaces than in those on DS surfaces (Fig. 1B).

SEM observation

To observe the mineral deposition and mineralized matrix formation on the experimental surfaces, the cellular layers were mechanically removed before specimen processing. After 4 weeks, mineral nodules were seen on both DS and OR FA surfaces with and even without MS. However, either with or without MS, more densely deposited nodules combined with a cellular matrix were observed on the OR FA surface compared with the DS one (Fig. 2). No SEM pictures of the SSE surface were able to be taken, as the whole surface layers were easily removed after the cells had been detached.

Alizarin red staining

After 4 weeks, without MS treatment, positive Alizarin red staining was seen in DPSCs grown on OR and DS surfaces, whereas no positive staining was observed in cells grown on SSE surfaces. With MS treatment, DPSCs grown on OR, DS, and SSE surfaces all displayed obvious Alizarin red staining. The staining intensity of cells grown on OR and DS surfaces was much stronger than that on SSE surfaces (Fig. 3). A subsequent quantitative osteogenesis assay was consistent with the results just cited (Fig. 4).

In vitro *tetracycline staining*

After being cultured with or without MS treatment on SSE and the FA-coated discs for 6 weeks, the cells grown on both the FA surfaces showed identifiable fluorescence staining for mineralized tissue formation. The OR FA stimulated evident mineralized tissue integration within the crystal layer, and this fluorescence staining, after being merged, overlapped with a similar obvious toluidine blue staining (Fig. 5). However, there was no identifiable staining for hard tissue formation in SSE groups and slightly positive fluorescence staining in DS surfaces with or without MS treatment (data not shown).

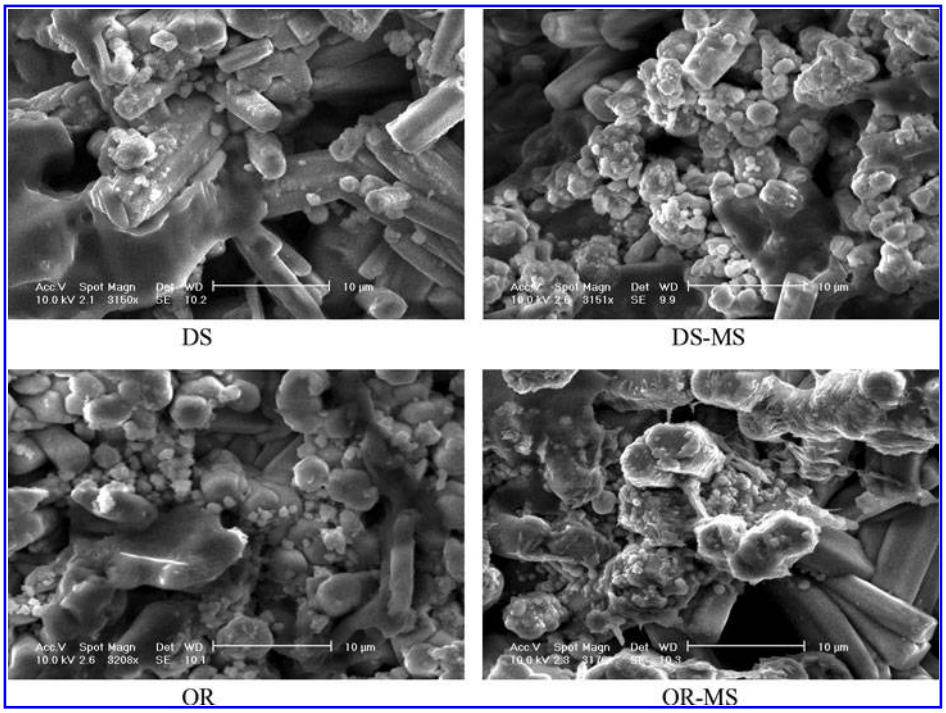

FIG. 2. Scanning electron micrograph of mineral nodule formation of DPSCs grown on OR and DS surfaces after treatment with or without MS for 4 weeks.

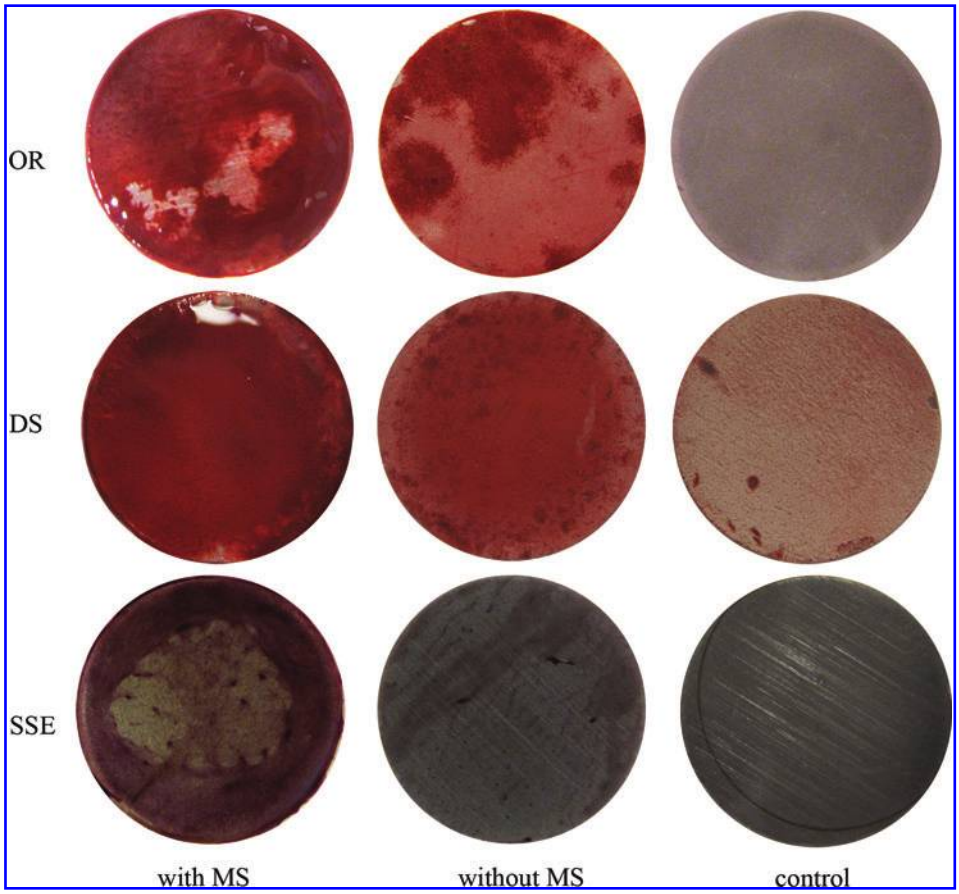

FIG. 3. Alizarin red staining of DPSCs grown on OR, DS, and SSE surfaces with or without MS treatment for 4 weeks. After 4 weeks, the cells grown on three different surfaces, with or without the addition of MS, were collected for Alizarin red staining according to the manufacturer's instructions (Osteogenesis Assay Kit, Millipore). Control, substrates only without cells. Color images available online at www.liebertpub.com/tec

Human pathway-focused osteogenesis PCR array analysis

Osteogenesis PCR array analysis was carried out to compare the gene profiles of DPSCs grown on SSE surfaces with that of the cells grown on OR and DS surfaces, with or without MS treatment at the time point of 4 weeks. We also compared the gene profile differences between the cells grown on the OR and DS FA surfaces at this time point.

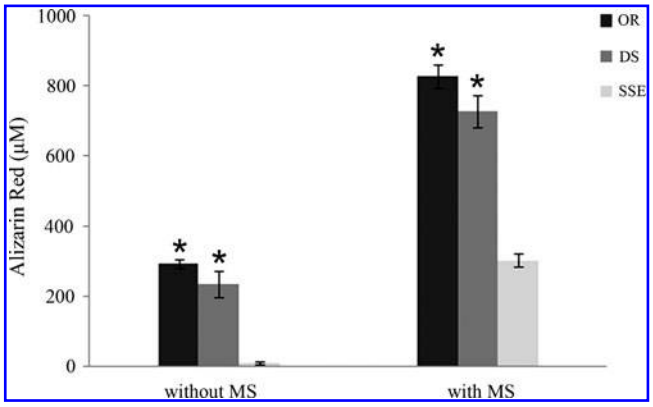

FIG. 4. Osteogenesis quantitative assay of DPSCs grown on OR, DS, and SSE surfaces with or without MS treatment for 4 weeks. After staining, the quantitative analysis was carried out through the extraction of Alizarin red from stained samples using acetic acid according to the manufacturer's protocols (Osteogenesis Assay Kit, Millipore). Three to five samples from each surface were used for one-way analysis of variance and Tukey's *post hoc* test, and significance was considered at $p < 0.05$. ($^*p < 0.05$).

Osteogenesis profiles of DPSCs grown on an OR FA crystal surface were carried out. Without MS, a total of 9 genes out of 84 genes were differentially regulated when the cells were grown on the OR compared with the SSE surface, with seven genes up-regulated and two genes down-regulated (Table 1A).

With MS, a total of 16 genes were differentially regulated when DPSCs were grown on an OR FA surface compared with those on the SSE surface. Fifteen genes were up-regulated, among which the expression of runt-related transcription factor 2 (*RUNX2*) was regulated with an over 1000-times fold change. The gene of fibroblast growth factor 2 (*FGF2*) was down-regulated in DPSCs grown on an OR FA surface (Table 1B).

Osteogenesis profiles of DPSCs grown on a DS FA crystal surface were carried out. Without MS, there were 16 genes differentially regulated when DPSCs were grown on the DS FA surface compared with those seeded on the SSE surface. A total of 10 genes were stimulated, including collagen, type X, alpha 1 (*COL10A1*) and phosphate-regulating endopeptidase homolog, Xlinked (*Phex*), and six genes inhibited by the DS FA surface (Table 2A).

With MS, a total of 17 genes were differentially regulated when DPSCs were grown on the DS FA surface compared with those on the SSE surface. Fourteen genes were up-regulated, with an 1139-times *RUNX2* up-regulation. The other three genes, bone morphogenetic protein 6 (*BMP6*),

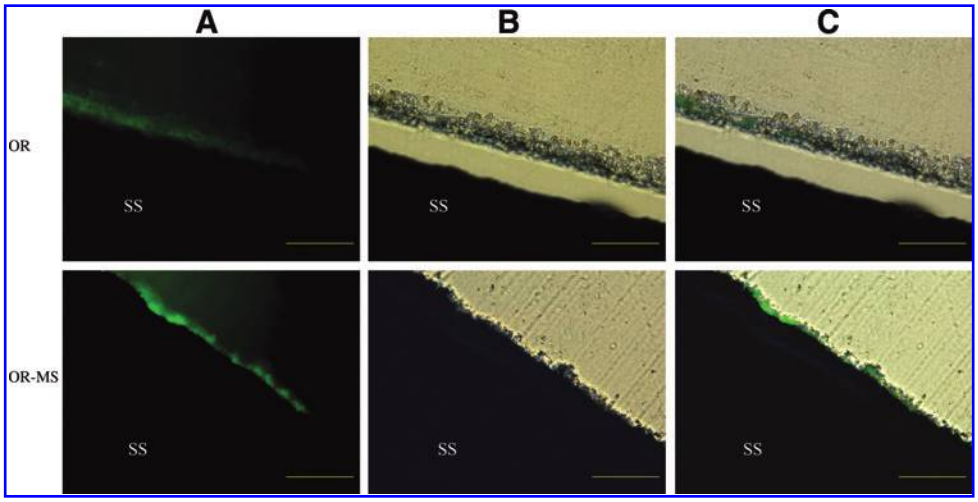

FIG. 5. Tetracycline fluorescence staining of DPSCs on OR FA surface with or without MS treatment for 6 weeks. **(A)** After DPSCs growing on OR FA surfaces with and without MS for 6 weeks, tetracycline, a bone fluorochrome was administered to label the newly formed bone-like mineralized tissue. **(B)** Toluidine blue was used to stain organic tissue components. **(C)** Merged pictures of staining A and B. Scale bar length: 200 μm. Color images available online at www.liebertpub.com/tec

Table 1A. Fold Change of the Human Pathway-Focused Osteogenesis Molecules Expressed by the Dental Pulp Stem Cells Grown on the Ordered Fluorapatite Surface Relative to the Etched Stainless Steel Surfaces at 4 Weeks (Without Mineralization Promoting Supplement)

Symbol	*Unigene*	*Ref. seq*	*Description*	*Fold change*
BGN	Hs.821	NM_001711	Biglycan	2.27
COL10A1	Hs.520339	NM_000493	Collagen, type X, alpha 1	6.88
COL15A1	Hs.409034	NM_001855	Collagen, type XV, alpha 1	2.33
COL3A1	Hs.443625	NM_000090	Collagen, type III, alpha 1	2.04
COMP	Hs.1584	NM_000095	Cartilage oligomeric matrix protein	3.87
ENAM	Hs.667018	NM_031889	Enamelin	1.92
PHEX	Hs.495834	NM_000444	Phosphate regulating endopeptidase homolog, X-linked	2.0
CD36	Hs.120949	NM_000072	CD36 molecule (thrombospondin receptor)	−2.94
ITGAM	Hs.172631	NM_000632	Integrin, alpha M (complement component 3 receptor 3 subunit)	−3.41

Table 1B. Fold Change of the Human Pathway-Focused Osteogenesis Molecules Expressed by the Dental Pulp Stem Cells Grown on the Ordered Fluorapatite Surface Relative to the Etched Stainless Steel Surfaces at 4 Weeks (With Mineralization Promoting Supplement)

Symbol	*Unigene*	*Ref. seq.*	*Description*	*Fold change*
AHSG	Hs.324746	NM_001622	Alpha-2-HS-glycoprotein	2.62
BMP4	Hs.68879	NM_130851	Bone morphogenetic protein 4	2.0
COL10A1	Hs.520339	NM_000493	Collagen, type X, alpha 1	13.57
COL11A1	Hs.523446	NM_080629	Collagen, type XI, alpha 1	3.12
DMP1	Hs.652366	NM_004407	Dentin matrix acidic phosphoprotein 1	6.83
ENAM	Hs.667018	NM_031889	Enamelin	5.11
FGF1	Hs.483635	NM_000800	Fibroblast growth factor 1 (acidic)	2.40
FGFR2	Hs.533683	NM_000141	Fibroblast growth factor receptor 2	2.21
ITGA1	Hs.644352	NM_181501	Integrin, alpha 1	2.12
MMP10	Hs.2258	NM_002425	Matrix metallopeptidase 10 (stromelysin 2)	3.32
MMP9	Hs.297413	NM_004994	Matrix metallopeptidase 9 (gelatinase B, 92 kDa gelatinase, 92 kDa type IV collagenase)	2.25
RUNX2	Hs.535845	NM_004348	Runt-related transcription factor 2	1153.66
SMAD1	Hs.604588	NM_005900	SMAD family member 1	2.48
STATH	Hs.654495	NM_003154	Statherin	4.67
TGFB3	Hs.592317	NM_003239	Transforming growth factor, beta 3	2.64
FGF2	Hs.284244	NM_002006	Fibroblast growth factor 2 (basic)	−2.62

After the real-time PCR amplification, relative gene expression values were analyzed using the Superarray web-based software package performing all $\Delta\Delta C_t$-based fold-change calculations.

PCR, polymerase chain reaction.

Table 2A. Fold Change of the Human Pathway-Focused Osteogenesis Molecules Expressed by the Dental Pulp Stem Cells Grown on the Disordered Fluorapatite Surface Relative to the Etched Stainless Steel Surfaces at 4 Weeks (Without Mineralization Promoting Supplement)

Symbol	*Unigene*	*Ref. seq.*	*Description*	*Fold change*
BGN	Hs.821	NM_001711	Biglycan	2.30
BMP5	Hs.296648	NM_021073	Bone morphogenetic protein 5	2.13
COL10A1	Hs.520339	NM_000493	Collagen, type X, alpha 1	15.05
COL15A1	Hs.409034	NM_001855	Collagen, type XV, alpha 1	2.50
COL3A1	Hs.443625	NM_000090	Collagen, type III, alpha 1	2.30
COMP	Hs.1584	NM_000095	Cartilage oligomeric matrix protein	4.83
FGF1	Hs.483635	NM_000800	Fibroblast growth factor 1 (acidic)	2.0
PHEX	Hs.495834	NM_000444	Phosphate regulating endopeptidase homolog, X-linked	2.0
TGFB1	Hs.645227	NM_000660	Transforming growth factor, beta 1	2.04
VDR	Hs.524368	NM_000376	Vitamin D (1,25-dihydroxyvitamin D3) receptor	2.04
ALPL	Hs.75431	NM_000478	Alkaline phosphatase, liver/bone/kidney	−2.01
BMP4	Hs.68879	NM_130851	Bone morphogenetic protein 4	−2.17
DMP1	Hs.652366	NM_004407	Dentin matrix acidic phosphoprotein 1	−3.89
DSPP	Hs.678914	NM_014208	Dentin sialophosphoprotein	−2.51
IGF2	Hs.523414	NM_000612	Insulin-like growth factor 2 (somatomedin A)	−2.41
ITGAM	Hs.172631	NM_000632	Integrin, alpha M (complement component 3 receptor 3 subunit)	−3.75

Table 2B. Fold Change of the Human Pathway-Focused Osteogenesis Molecules Expressed by the Dental Pulp Stem Cells Grown on the Disordered Fluorapatite Surface Relative to the SSE Surfaces at 4 Weeks (With Mineralization Promoting Supplement)

Symbol	*Unigene*	*Ref. seq.*	*Description*	*Fold change*
AHSG	Hs.324746	NM_001622	Alpha-2-HS-glycoprotein	2.05
COL10A1	Hs.520339	NM_000493	Collagen, type X, alpha 1	14.36
COL11A1	Hs.523446	NM_080629	Collagen, type XI, alpha 1	2.0
DMP1	Hs.652366	NM_004407	Dentin matrix acidic phosphoprotein 1	2.23
ENAM	Hs.667018	NM_031889	Enamelin	3.93
FGF1	Hs.483635	NM_000800	Fibroblast growth factor 1 (acidic)	2.74
IGF1	Hs.160562	NM_000618	Insulin-like growth factor 1 (somatomedin C)	2.40
IGF1R	Hs.643120	NM_000875	Insulin-like growth factor 1 receptor	2.06
ITGA1	Hs.644352	NM_181501	Integrin, alpha 1	2.09
MMP8	Hs.161839	NM_002424	Matrix metallopeptidase 8 (neutrophil collagenase)	2.70
MMP9	Hs.297413	NM_004994	Matrix metallopeptidase 9 (gelatinase B, 92 kDa gelatinase, 92 kDa type IV collagenase)	2.0
RUNX2	Hs.535845	NM_004348	Runt-related transcription factor 2	1139.35
SMAD1	Hs.604588	NM_005900	SMAD family member 1	2.50
STATH	Hs.654495	NM_003154	Statherin	2.18
BMP6	Hs.285671	NM_001718	Bone morphogenetic protein 6	−2.21
CD36	Hs.120949	NM_000072	CD36 molecule (thrombospondin receptor)	−4.31
FGF2	Hs.284244	NM_002006	Fibroblast growth factor 2 (basic)	−2.21

After the real-time PCR amplification, relative gene expression values were analyzed using the Superarray web-based software package performing all $\Delta\Delta C_t$-based fold-change calculations.

FGF2, and *CD36*, were down-regulated in DPSCs grown on the DS FA surface with MS treatment (Table 2B).

Osteogenesis profiles of DPSCs grown on OR and DS FA crystal surfaces were carried out. Without MS, a total of four genes were differentially regulated when DPSCs were grown on an OR FA surface compared with those on the DS FA surface. *BMP4*, dentin matrix acidic phosphoprotein 1 (*DMP1*), and dentin sialophosphoprotein (*DSPP*) were up-regulated, while *COL10A1* was down-regulated (Table 3A).

With MS, a total of seven genes were differentially regulated. The OR FA stimulated six genes, including *DMP1*, matrix metallopeptidase 10 (*MMP10*), and transforming growth factor, beta 3 (*TGFβ3*). The Fms-related tyrosine kinase 1 (*FLT1*) was down-regulated (Table 3B).

Discussion

In our laboratory, we have synthesized a highly orientated FA film with a prism-like structure that is similar to human enamel. As is well known, natural bone accumulates fluoride ions from the blood, forming a fluoride containing HA. Fluoride ions within the lattice replace hydroxide ions, creating a tighter lattice structure. It is, thus, possible that this FA crystal scaffold could also be applied for various orthopaedic applications. In our previous article, we have discussed the use of the OR FA films as surface preparations that encourage bony integration in dental and orthopedic applications.[5,7] In this study, we used this enamel-like surface structure as a biomimetic interface between the FA crystals and the DPSCs

Table 3A. Fold Change of the Human Pathway-Focused Osteogenesis Molecules Expressed by the Dental Pulp Stem Cells Grown on the Ordered Fluorapatite Surface Relative to the Disordered Surfaces at 4 Weeks (Without Mineralization Promoting Supplement)

Symbol	*Unigene*	*Ref. seq.*	*Description*	*Fold change*
BMP4	Hs.68879	NM_130851	Bone morphogenetic protein 4	2.45
DMP1	Hs.652366	NM_004407	Dentin matrix acidic phosphoprotein 1	3.18
DSPP	Hs.678914	NM_014208	Dentin sialophosphoprotein	2.0
COL10A1	Hs.520339	NM_000493	Collagen, type X, alpha 1	2.19

Table 3B. Fold Change of the Human Pathway-Focused Osteogenesis Molecules Expressed by the Dental Pulp Stem Cells Grown on the Ordered Fluorapatite Surface Relative to the Disordered Surfaces at 4 Weeks (With Mineralization Promoting Supplement)

Symbol	*Unigene*	*Refseq*	*Description*	*Fold change*
BMP6	Hs.285671	NM_001718	Bone morphogenetic protein 6	2.0
CD36	Hs.120949	NM_000072	CD36 molecule (thrombospondin receptor)	8.39
DMP1	Hs.652366	NM_004407	Dentin matrix acidic phosphoprotein 1	3.07
MMP10	Hs.2258	NM_002425	Matrix metallopeptidase 10 (stromelysin 2)	2.43
STATH	Hs.654495	NM_003154	Statherin	2.14
TGFB3	Hs.592317	NM_003239	Transforming growth factor, beta 3	2.0
FLT1	Hs.654360	NM_002019	Fms-related tyrosine kinase 1 (vascular endothelial growth factor/vascular permeability factor receptor)	−2.22

After the real-time PCR amplification, relative gene expression values were analyzed using the Superarray web-based software package performing all $\Delta\Delta C_t$ based fold-change calculations.

to investigate its influence on their differentiation and mineralization. This was an attempt to establish the FA surfaces as a scaffold for dentin and pulp regeneration and, potentially, as a simple biomimetic model for the creation of an enamel/dentin/pulp complex of the tooth.

As in tissue engineering, the well-designed, biomimetic biomaterials or scaffolds are crucial in determining and/or directing the pathway of recruited stem cell differentiation and related new tissue regeneration. Earlier, it was demonstrated that molecules solubilized from the dentin are key in promoting the DPSCs to differentiate and produce a mineralized dentin-like tissue.[8] In the present study, ALP staining was carried out to show the differentiation of DPSCs, as ALP expression is widely accepted as an earlier marker for the differentiation of cells forming hard tissues. However, Alizarin red staining, as well as its related osteogenesis quantitative assay, and tetracycline staining were used to study the late-stage mineralized tissue formation. These results, along with the SEM observation showing mineral nodule formation, suggested that, even without treatment by dentinal soluble molecules or by an MS, DPSCs grown on enamel-like FA surfaces were capable of differentiating into mineralized tissue forming cells and undergoing a subsequent mineralization process. This is consistent with our previous work showing that MG-63 cells grown on the FA surface were able to differentiate and mineralize even without OI.[7]

The osteogenesis gene profile analysis was performed to help us explain the mechanisms underlying this DPSC differentiation and mineralization process. As shown in the results, the FA crystal surfaces stimulated the expression of several collagen genes, including collagen type X, XI, and XV with or without MS treatment. A previous study has shown that mutations of collagen type XI resulted in severe abnormalities of bone, which would usually lead to the death of the animals at birth. It was suggested that collagen type XI may have an important function in solid connective tissue development.[9] The up-regulation of collagen type XI and the other collagen genes by the OR FA surfaces are likely to provide a favorable microenvironment for the differentiation of DPSCs with or even without MS treatment.

The Phex, a transmembrane metalloendoprotease, is found to be predominantly localized in teeth and bone. Since it is critical to the process of bone mineralization, it is commonly thought to be one of the required genes for normal bone formation and the process of biomineralization.[10,11] Without MS treatment, a similar up-regulation of *Phex* expression was detected on both OR and DS FA surfaces compared with the SSE surface. This would suggest that both OR and DS FA surfaces may stimulate biomineralization through enhanced *Phex* expression.

With MS, it is most noticeable that *Runx2* is significantly up-regulated in cells grown on both OR and DS FA surfaces. Runx2, a downstream target of BMP signaling, is a master transcription factor of the bone that is necessary for the differentiation of pluripotent mesenchymal cells to osteoblasts. Runx2 is required in maintaining fully functional cells and is essential for the initial commitment of mesenchymal cells to the osteoblastic lineage. Runx2 also controls the proliferation, differentiation, and maintenance of these cells.[12–14] Runx2 is affected by a diversity of signaling pathways. The binding of extracellular matrix (ECM) proteins to cell-surface integrins, FGF2, and BMPs influences Runx2-dependent transcription.[15,16] Runx2 has also been suggested to be essential for tooth development.[17,18] It is increasingly expressed in early odontoblasts, but is either low or undetectable in differentiated odontoblasts.[19,20] Interestingly, Runx2 increased *DSPP* expression in immature odontoblasts, but down-regulated its expression in more mature cells, showing that the effect of

Runx2 is dependent on the state of differentiation of the target cells.[21]

Among numerous ECM molecules, DMP1 is a bone-, as well as a tooth, specific protein. It was initially identified from mineralized dentin and is believed to be involved in the regulation of mineralization and apatite deposition.[22] DMP1 is crucial in the maturation of odontoblasts and osteoblasts and in the biomineralization process.[23] In the dentin–pulp complex, DMP1 can act as a morphogen in undifferentiated mesenchymal cells, and induce the odontoblast differentiation of DPSCs, as well as dentin-like tissue regeneration.[24] In addition, DMP1 has been shown to nucleate apatite crystals and to induce dentin formation.[25] Both DMP1 and Phex are significantly involved in maintaining appropriate serum phosphate levels required for the normal mineralization of teeth and bone.[26] In our study, without MS treatment, the *DMP1* expression was 3.8-fold inhibited in DPSCs on a DS FA surface, while with MS treatment, it was greatly up-regulated on both OR and DS FA surfaces compared with the SSE surface. With or without MS treatment, the up-regulation of *DMP1* was shown in cells grown on an OR FA surface compared with those on a DS FA surface. Since DMP1 is considered one of the key phenotypic mineralization markers, this result was in accordance with the mineralization data, which detected much more mineral formation on OR FA surfaces than on DS FA surfaces with or without MS. In addition, with MS, the enhanced *DMP1* expression is consistent with the stronger tetracycline staining of the new mineral formation on FA surfaces.

In our study, the *BMP4* and *SMAD1* expression of DPSCs grown on FA surfaces was enhanced with MS treatment, but the expression of *BMP4* was inhibited in the cells on DS FA surfaces. Promisingly, the *BMP4* and *BMP6* expression was up-regulated in cells grown on an OR FA surface compared with those on DS FA. Earlier studies demonstrated that BMPs trigger signaling events which induce dentin formation in animal models.[27,28] Among the 15 known human BMPs, BMP4 has been shown to induce undifferentiated mesenchymal stem cells to differentiate into chondroblasts or osteoblasts.[29]

In a previous study, the activation of insulin-like growth factor (IGF) and epidermal growth factor (EGF) pathways has been proved to be closely related to the osteogenesis induction of BMP6,[30] whereas, in our study, the up-regulation of *IGF1* was coordinated with the down-regulation of *BMP6* in MS-treated groups, suggesting that other BMPs members and growth factors may be actively involved in the activation of IGF pathways. Compared with the SSE group, the expression of *FGF1* was stimulated on both the OR and DS FA surfaces, whereas the *FGF2* were inhibited on FA surfaces with MS treatment, indicating the involvement of FGF signaling pathway during this process. Significantly, FGF1 has been shown to have duel effects on favoring both angiogenesis and osteogenesis, which are crucial in the physiology of the bone development and repair process.[31] Moreover, our study showed the up-regulation of growth factors such as TGFβ1 and TGFβ3 by the FA surfaces with or without MS. This is consistent with a previous study that the TGFβ and FGF family genes appear to be vital in mediating the odontoblast differentiation process.[32]

It is also noteworthy that DPSCs behavior differed when seeded on the OR and DS FA surfaces, suggesting that the surface topography of the FA substrate could affect this apatite-directed cell initial adhesion, growth and differentiation, and related mineralization process.[5,7] It is now well accepted that besides the intrinsic characteristics of a substrate, for example, chemical compositions, charge, and hydrophobicities, the topographical features such as mechanics and the geometric microenvironment also show the potential to direct cell responses, including different cell fate selections. Discher reviewed the response of various cells on different stiffness of a substrate, implying this physical property modulates cell or tissue development, differentiation, and the regeneration process. Moreover, Vogel and Sheetz' review reported the capabilities of cells in sensing the force or geometry of a material, such as substrate rigidity and microstructure, to transfer these physical and geometrical signals into cellular biochemical signals that regulate various cellular activities. Poellmann *et al.* also showed cell morphological changes to different geometric microenvironments using quantitative measurements.[33–35] Consistently, our results suggested that different cellular behaviors and biological responses are probably due to the topographically different microenvironment.

In summary, we demonstrated that FA crystal surfaces, especially the OR FA surface, mimicked the physical architecture of enamel, and provided a favorable extracellular microenvironment for the cells. Moreover, it induced and stimulated the differentiation of human DPSCs and mineralized tissue formation without an MS compared with an uncoated metal surface. This demonstrates the promising advantages of FA surfaces as a simple biomimetic model for dentin regeneration, enamel/dentin/pulp complex creation, and as a scaffold for hard tissue engineering.

Acknowledgment

This study was supported by NIH grants DE020983.

Disclosure Statement

No competing financial interests exist.

References

1. Yen, A.H., and Sharpe, P.T. Stem cells and tooth tissue engineering. Cell Tissue Res **331,** 359, 2008.
2. Gronthos, S., Mankani, M., Brahim, J., Robey, P.G., and Shi, S. Postnatal human dental pulp stem cells (DPSCs) *in vitro* and *in vivo*. Proc Natl Acad Sci U S A **97,** 13625, 2000.
3. Gronthos, S., Brahim, J., Li, W., Fisher, L.W., Cherman, N., Boyde, A., DenBesten, P., Robey, P.G., and Shi, S. Stem cell properties of human dental pulp stem cells. J Dent Res **81,** 531, 2002.
4. Chen, H.F., Tang, Z.Y., Liu, J., Sun, K., Chang, S.R., Peters, M.C., Mansfield, J.F., Czajka-Jakubowska, A., and Clarkson, B.H. A cellular synthesis of a human enamel-like microstructure. Adv Mater **18,** 1846, 2006.
5. Liu, J., Jin, T.C., Chang, S., Czajka-Jakubowska, A., and Clarkson, B.H. Adhesion and growth of dental pulp stem cells on enamel-like fluorapatite surfaces. J Biomed Mater Res A **96,** 528, 2011.
6. Liu, J., Jin, T., Ritchie, H.H., Smith, A.J., and Clarkson, B.H. *In vitro* differentiation and mineralization of human dental pulp cells induced by dentin extract. In Vitro Cell Dev Biol **41,** 232, 2005.
7. Liu, J., Jin, T., Chang, S., Czajka-Jakubowska, A., Zhang, Z., Nör, J.E., and Clarkson, B.H. The effect of novel fluorapatite surfaces on osteoblast-like cell adhesion, growth, and mineralization. Tissue Eng Part A **16,** 2977, 2010.

8. Demarco, F.F., Casagrande, L., Zhang, Z., Dong, Z., Tarquinio, S.B., Zeitlin, B.D., Shi, S., Smith, A.J., and Nör, J.E. Effects of morphogen and scaffold porogen on the differentiation of dental pulp stem cells. J Endod **36,** 1805, 2010.
9. Li, Y., Lacerda, D.A., Warman, M.L., Beier, D.R., Yoshioka, H., Ninomiya, Y., Oxford, J.T., Morris, N.P., Andrikopoulos, K., Ramirez, F., *et al.* A fibrillar collagen gene, Col11a1, is essential for skeletal morphogenesis. Cell **80,** 423, 1995.
10. Ruchon, A.F., Tenenhouse, H.S., Marcinkiewicz, M., Siegfried, G., Aubin, J.E., Desgroseillers, L., Crine, P., and Boileau, G. Developmental expression and tissue distribution of Phex protein: effect of the Hyp mutation and relationship to bone markers. J Bone Miner Res **15,** 1440, 2000.
11. Miao, D., Bai, X., Panda, D., McKee, M., Karaplis, A., and Goltzman, D. Osteomalacia in hyp mice is associated with abnormal phex expression and with altered bone matrix protein expression and deposition. Endocrinology **142,** 926, 2001.
12. Ducy, P., Zhang, R., Geoffroy, V., Ridall, A.L., and Karsenty, G. Osf2/Cbfa1: a transcriptional activator of osteoblast differentiation. Cell **89,** 747, 1997.
13. Ducy, P., Starbuck, M., Priemel, M., Shen, J., Pinero, G., Geoffroy, V., Amling, M., and Karsenty, G.A. Cbfa1-dependent genetic pathway controls bone formation beyond embryonic development. Genes Dev **13,** 1025, 1999.
14. Quack, I., Vonderstrass, B., Stock, M., Aylsworth, A.S., Becker, A., Brueton, L., Lee, P.J., Majewski, F., Mulliken, J.B., Suri, M., Zenker, M., Mundlos, S. and Otto, F. Mutation analysis of core binding factor A1 in patients with cleidocranial dysplasia. Am J Hum Genet **65,** 1268, 1999.
15. Franceschi, R.T., Xiao, G., Jiang, D., Gopalakrishnan, R., Yang, S., and Reith, E. Multiple signaling pathways converge on the Cbfa1/Runx2 transcription factor to regulate osteoblast differentiation. Connect Tissue Res **44,** 109, 2003.
16. Franceschi, R.T., and Xiao, G. Regulation of the osteoblastspecific transcription factor, Runx2: responsiveness to multiple signal transduction pathways. J Cell Biochem **88,** 446, 2003.
17. D'Souza, R.N., Aberg, T., Gaikwad, J., Cavender, A., Owen, M., Karsenty, G., and Thesleff, I. Cbfa1 is required for epithelial–mesenchymal interactions regulating tooth development in mice. Development **126,** 2911, 1999.
18. Aberg, T., Cavender, A., Gaikwad, J.S., Bronckers, A.L., Wang, X., Waltimo-Siren, J., Thesleff, I., and D'Souza, R.N. Phenotypic changes in dentition of Runx2 homozygote-null mutant mice. J Histochem Cytochem **52,** 131, 2004.
19. Bronckers, A.L., Engelse, M.A., Cavender, A., Gaikwad, J., and D'Souza, R.N. Cell-specific patterns of Cbfa1 mRNA and protein expression in postnatal murine dental tissues. Mech Dev **101,** 255, 2001.
20. Liu, H., Li, W., Shi, S., Habelitz, S., Gao, C., and Denbesten, P. MEPE is downregulated as dental pulp stem cells differentiate. Arch Oral Biol **50,** 923, 2005.
21. Chen, S., Rani, S., Wu, Y., Unterbrink, A., Gu, T.T., Gluhak-Heinrich, J., Chuang, H.H., and MacDougall, M. Differential regulation of dentin sialophosphoprotein expression by Runx2 during odontoblast cytodifferentiation. J Biol Chem **280,** 29717, 2005.
22. George, A., Sabsay, B., Simonian, P.A., and Veis, A. Characterization of a novel dentin matrix acidic phosphoprotein. Implications for induction of biomineralization. J Biol Chem **268,** 12624, 1993.
23. Qin, C., D'Souza, R., and Feng, J.Q. Dentin matrix protein 1 (DMP1): new and important roles for biomineralization and phosphate homeostasis. J Dent Res **86,** 1134, 2007.
24. Almushayt, A., Narayanan, K., Zaki, A.E., and George, A. Dentin matrix protein 1 induces cytodifferentiation of dental pulp stem cells into odontoblasts. Gene Ther **13,** 611, 2006.
25. He, G., Dahl, T., Veis, A., and George, A. Nucleation of apatite crystals *in vitro* by self-assembled dentin matrix protein 1. Nat Mater **2,** 552, 2003.
26. Gorski, J.P., Huffman, N.T., Chittur, S., Midura, R.J., Black, C., Oxford, J., and Seidah, N.G. Inhibition of proprotein convertase SKI-1 blocks transcription of key extracellular matrix genes regulating osteoblastic mineralization. J Biol Chem **286,** 1836, 2011.
27. Nakashima, M. Induction of dentine in amputated pulp of dogs by recombinant human bone morphogenetic proteins-2 and −4 with collagen matrix. Arch Oral Biol **39,** 1085, 1994.
28. Rutherford, R.B., Wahle, J., Tucker, M., Rueger, D., and Charette, M. Induction of reparative dentine formation in monkeys by recombinant human osteogenic protein-1. Arch Oral Biol **38,** 571, 1993.
29. Marsell, R., and Einhorn, T.A. The role of endogenous bone morphogenetic proteins in normal skeletal repair. Injury **40,** S4, 2009.
30. Grasser, W.A., Orlic, I., Borovecki, F., Riccardi, K.A., Simic, P., Vukicevic, S., and Paralkar, V.M. BMP-6 exerts its osteoinductive effect through activation of IGF-I and EGF pathways. Int Orthop **31,** 759, 2007.
31. Kelpke, S.S., Zinn, K.R., Rue, L.W., and Thompson, J.A. Site-specific delivery of acidic fibroblast growth factor stimulates angiogenic and osteogenic responses *in vivo*. J Biomed Mater Res A **71,** 316, 2004.
32. Ruch, J.V., Lesot, H., and Begue-Kirn, C. Odontoblast differentiation. Int J Dev Biol **39,** 51, 1995.
33. Poellmann, M.J., Harrell, P.A., King, W.P., and Wagoner Johnson, A.J. Geometric microenvironment directs cell morphology on topographically patterned hydrogel substrates. Acta Biomater **6,** 3514, 2010.
34. Discher, D.E., Janmey, P., and Wang, Y.L. Tissue cells feel and respond to the stiffness of their substrate. Science **310,** 1139, 2005.
35. Vogel, V., and Sheetz, M. Local force and geometry sensing regulate cell functions. Nat Rev Mol Cell Biol **7,** 265, 2006.

Address correspondence to:
Jun Liu, Ph.D.
Department of Cariology, Restorative Sciences and Endodontics
2310 I Dental School
University of Michigan
1011 N. University Ave.
Ann Arbor, MI 48109

E-mail: junlc@umich.edu

Longxing Ni, Ph.D.
Department of Operative Dentistry and Endodontics
School of Stomatology
Fourth Military Medical University
No. 145 Western Changle Road, Xi'an
Shaanxi 710032
P.R. China

E-mail: nilx2007@gmail.com

Received: November 3, 2011
Accepted: May 1, 2012
Online Publication Date: June 15, 2012

This article has been cited by:

1. Gokul Gopinathan, Antonia Kolokythas, Xianghong Luan, Thomas G.H. Diekwisch. 2013. Epigenetic Marks Define the Lineage and Differentiation Potential of Two Distinct Neural Crest-Derived Intermediate Odontogenic Progenitor Populations. *Stem Cells and Development* **22**:12, 1763-1778. [Abstract] [Full Text HTML] [Full Text PDF] [Full Text PDF with Links] [Supplemental Material]